HOXC6 Promotes Metastasis of MSI-H CRC via Interacting with M2 Macrophages

lina qi
Zhejiang University School of Medicine
biting zhou
Zhejiang University School of Medicine
jiani chen
Zhejiang University School of Medicine
kailun xu
Zhejiang University School of Medicine
kailai wang
Zhejiang University School of Medicine
shu zheng
Zhejiang University School of Medicine
wangxiong hu (wxhu@zju.edu.cn)
Zhejiang University School of Medicine https://orcid.org/0000-0002-2287-9242

Research

Keywords: colorectal cancer, EMT, HOXC6, MSI-H, tumor-associated macrophages

Posted Date: November 19th, 2020

DOI: https://doi.org/10.21203/rs.3.rs-108058/v1

Abstract

Background: *HOXC6* was the most significantly upregulated gene in right-sided colon cancer (RCC) compared to left-sided colon cancer (LCC) according to our previous study. It is known that RCC has a higher immunogenicity than LCC because much higher prevalence of MSI-H samples, however, the role of HOXC6 acted in MSI-H tumors remains poorly understood.

Methods: Expression datasets from The Cancer Genome Atlas (TCGA) and Gene Expression Omnibus databases were used to analyze the differential expression and prognostic role of HOXC6 in CRC. ELISA and qRT-PCR were performed to examine the association of HOXC6 and CCL2. Immunohistochemistry and immunofluorescence were performed to evaluate the correlation of HOXC6 and M2 macrophage infiltration. CCK8 and Transwell were used to evaluate the proliferation and migration of tumor cells *in vitro*.

Results: HOXC6 was overexpressed in MSI-H CRC and associated with poor prognosis. Upregulation of CCL2 by HOXC6 could attract more M2 macrophage infiltration. IL6 secreted by M2 macrophages could induce epithelial-mesenchymal transition (EMT) of tumor cells by upregulating HOXC6. Overexpression of HOXC6 promoted the migration and invasion of CRC cells *in vitro*. Finally, inhibition of IL6/JAK pathway using ruxolitinib downregulated HOXC6 and suppressed invasion of HCT116 cells.

Conclusion: Our study revealed that overexpression of HOXC6 attracted more M2 macrophage infiltration and the positive crosstalk between M2 macrophages and HOXC6-highly expressed tumor led to EMT and enhanced the migration ability of CRC, which offered a promising therapic target for treatment of MSI-H CRC.

Introduction

Colorectal cancer (CRC) is one of the most common diagnosed malignant tumors, with the third morbidity and mortality among all malignant tumors in the United States [1]. Liver metastasis is observed in more than half CRC patients and less than 20% of newly diagnosed metastatic CRC patients survive more than five years [2]. This situation highlights the pressing need to better understanding of metastatic development and better controlling of tumor progression in CRC.

In recent years, a bunch of studies have revealed that right-sided colon cancer (RCC) has a higher immunogenicity than left-sided colon cancer (LCC) because much higher microsatellite instability-high (MSI-H) frequency and better response to anti-PD-1/PD-L1 immunotherapies [3–5]. Though generally MSI-H confers CRC patients a favorable outcome, stage IV MSI-H CRC patients have a worse prognosis than microsatellite stable (MSS) patients (11.1 months vs. 22.1 months, $P = 0.017$) [6], with the mechanism remains poorly understood. We previous found MLH1 inactivation upregulates HOXC6 moderately, suggesting that other than intratumor per se, stromal or immune cells within tumor microenvironment (TME) may also has a role in regulating tumoral HOXC6 expression.

In this study, we confirmed that HOXC6 was overexpressed in MSI-H CRC and associated with a worse prognosis. Furthermore, we discovered a novel association between HOXC6 overexpressed CRC cells and M2 macrophages using bioinformatic exploration coupled with experimental validation. Upregulation of CCL2 by HOXC6 in tumor cells attracted more M2 infiltration within TME. Additionally, the regulatory axis IL6/HOXC6 in CRC cells contributing to EMT induced by M2 macrophages was identified and inhibition of HOXC6 signaling cascade by targeting IL6/JAK pathway suppressed EMT, which helped to better understand the crosstalk between CRC and tumor associated macrophages (TAM) and offered a good candidate target in CRC treatment.

Materials And Methods

Bioinformatic analysis of TCGA and GEO datasets

All Level 3 CRC RNASeqV2 mRNA expression profiles were obtained from TCGA (08/26, 2017). The raw CEL files of GSE39582 (Affymetrix HG U133 Plus 2.0 arrays) were downloaded from Gene Expression Omnibus (GEO) and processed using the *affy* package of BioConductor [10]. Then, the MAS5 algorithm was used for background correction, normalization and summarization of single probes for all probe sets. The identification of differentially expressed genes (DEGs) between subgroups was performed as in our previous studies [7, 8]. Significant DEGs were selected according to a false discovery rate (FDR) adjusted *P*-value < 0.05 and fold change > 2. Gene Ontology (GO) and Kyoto Encyclopedia of Genes and Genomes (KEGG) enrichment analyses were performed using the *clusterProfiler* package from Bioconductor based on the DEGs identified between the HOXC6+ (> median) and HOXC6- (< median) groups [9]. Significantly enriched GO terms and pathways were selected according to a FDR-adjusted *P*-value < 0.01. Hallmark gene sets from the molecular signatures database (MSigDB) [10] were used to determine whether any signatures were enriched in specific groups by gene set enrichment analysis (GSEA) [11]. Significantly enriched hallmarks were chosen according to a *P*-value < 0.05.

To quantify the relative amount of distinct lymphocytes in CRC, CIBERSORT [12] was used to calculate the proportions of 22 lymphocytes in tumor tissue. The permutation was set to ≥ 100, and quantile normalization of the input expression mixture was set to FALSE for TCGA RNAseq dataset. Samples with a *P*-value > 0.05 were excluded from further comparisons. Consensus tumor purity was refined based on a previous systematic pan-cancer measurement of tumor purity [13].

Immunofluorescence (IF) staining and calculation of CD206-positive area

A total of 53 stage II RCC samples collected from Zhejiang University Cancer Institute (ZUCI) were used for IF staining to evaluate the expression of CD206 (a marker of M2 macrophages). Written informed consent was obtained from all patients before enrolment. A primary antibody against CD206 (1:200, HUABIO, ET1702-04) was used for IF staining. ImageJ was used to calculate the CD206-positive area percentage. In brief, the image was separated based on the channels and displayed as 8-bit images.

Then, the threshold was adjusted. The areas of DAPI (nuclear location) and CD206 were calculated. The percentage of CD206-positive area was calculated as (CD206-positive area)/(DAPI-positive area).

Cell culture and coculture

The HCT116 and THP-1 cell lines were purchased from ATCC and cultured with RPMI 1640 medium (Gibco) containing 10% fetal bovine serum (FBS, BI Industry). The cells were incubated at 37℃ with 5% CO_2. M2 macrophages were generated from THP-1 cells *in vitro*. Briefly, THP-1 cells were first treated with 200 nM PMA (Sigma-Aldrich, Catalog Number: P1585) for 24 h to differentiate into macrophages. Then, 20 ng/ml IL-4 (Sigma-Aldrich, Catalog Number: SRP4137) and 20 ng/ml IL-13 (PeproTech, Catalog Number: 200 − 13) were added for 48 h to induce M2 macrophages.

Cocultivation of macrophages and HCT116 cells was conducted with the noncontact coculture Transwell system (Corning, USA). Inserts containing 1.0×10^6 THP-1 cells or M2 macrophages were transferred to 6-well plates previously seeded with HCT116 cells (2.5×10^5 cells per well) and cocultured in 1.5% FBS-containing medium for 72 h. HCT116, THP-1, or M2 macrophages were cultured in 1.5% FBS-containing medium as a negative control. After coculture, macrophages, HCT116 cells and culture medium were harvested for use. IL6 was purchased from PeproTech (Catalog Number: 200-06).

Stable gene overexpression using the lentiviral transfection system

LV-HOXC6 (Gene, Shanghai, 24024-1) and negative control lentivirus (CON238) were purchased from GeneChem (Shanghai, China). For infection, 10^5 cells were plated into 6-well plates and cocultured with 2.5×10^6 transducing-units (TU) virus in the presence of 1X Hitrans G (GeneChem, Shanghai, China) and standard medium. Twelve to15 hours later, the medium was replaced with fresh complete culture medium. After 72 h of transfection, 2 mg/ml or 8 mg/ml puromycin was added to the culture medium for HCT116 selection, respectively. Western blot and quantitative reverse transcription-polymerase chain reaction (qRT-PCR) were utilized to confirm HOXC6 overexpression.

siRNA knockdown

Cells were plated into 6-well plates. After the cells grew to 50–60% confluence, Lipo 3000 (Invitrogen) with specific siRNA (Genepharma, Shanghai) was added to the cells according to the manufacturer's suggestions. The final concentration of siRNA was 100 nM. Cells were incubated with siRNA for 48 h and then harvested for protein and RNA extraction. The sequences of *HOXC6* siRNA were as follows: sense: 5'-GAAAGCCAGUAUCCAGAUUTT-3' and antisense: 5'-AAUCUGGAUACUGGCUUUCTT-3'. The sequences of *IL6* siRNA were as follows: sense: 5'-CCCAGGAGAAGAUUCCAAATT-3' and antisense: 5'-UUUGGAAUCUUCUCCUGGGTT-3'. The negative control siRNA sequences were as follows: sense: 5'-UUCUCCGAACGUGUCACGUTT-3' and antisense: 5'-ACGUGACACGUUCGGAGAATT-3'.

Transwell migration assays

Cell migration was examined by Transwell assays without Matrigel. Approximately 10^4 cells were plated into the upper chamber with RPMI 1640 medium without FBS. RPMI 1640 medium supplemented with 20% FBS was added to the lower chamber. After 48 h of culture for HCT116 cells, the cells in the upper chamber were scarpered, and cells under the upper chamber were fixed with 4% formalin and stained with crystal violet. The migrated cells were counted by light microscopy, and the mean cell number of three random visual fields at a magnification of 200 × was recorded.

Cell proliferation

Approximately 1×10^3 cells were plated into 96-well plates. Cell viability was measured at 1, 3, 5, and 7 days after plating. Cell Counting Kit-8 (CCK-8, Dojindo, Japan, CK04) was utilized for cell viability testing. Cell culture medium was used as a blank control. After 2–3 hours of incubation, an optimal density (OD) value of 450 nm was used to detect cell proliferation. Experiments were carried out in triplicate. Ruxolitinib were purchased from Selleck.

Protein extraction and western blotting

RIPA buffer (Beyotime) with 1% protease inhibitor cocktail (Roche Applied Science) was used for total protein extraction. After quantification of protein concentration and boiling with protein loading buffer, 10% SDS-polyacrylamide gel electrophoresis (SDS-PAGE) gels were used to separate proteins and polyvinylidene fluoride (PVDF) membranes by electrophoresis were used for protein transition. After blocking with 5% nonfat milk, the PVDF membranes were incubated with primary antibodies followed by horseradish peroxidase (HRP)-linked secondary antibodies. Enhanced chemiluminescence (ECL) reagent was used to detect the protein bands. The primary antibodies used for western blotting were as follows: anti-HOXC6 (Santa Cruz, sc-376330), anti-EMT antibody kit (Cell Signaling Technology, #9782), anti-IL6 (Abcam, ab233551), and anti-β-tubulin (Huabio, Hangzhou, M1305-2). β-tubulin was used as a protein loading control.

RNA isolation and qRT-PCR

Total RNA was extracted from HCT116 cells using Trizol following a standard protocol. The Takara PrimeScript TM RT Master Mix Kit (Takara, RR036Q) was used for reverse transcription. The iTaq Universal SYBR Green Supermix (BioRad) and Applied Biosystems 7500 Fast Real-Time PCR System were applied for qRT-PCR. GAPDH was used as the loading control. Experiments were carried out in triplicate. The results were calculated as follows: $\Delta CT = CT_{Experimental/NC} - CT_{GAPDH}$, $\Delta\Delta CT = \Delta CT_{Experimental/NC} - \Delta CT_{NC,}$ fold change = $2^{-\Delta\Delta CT}$. The primers used for qRT-PCR are as follows.

	Forward sequence (5′ to 3′)	Reverse sequence (5′ to 3′)
HOXC6	GAGAATGTCGTGTTCAGTTC	GATCTGTCGCTCGGTCAGGCAA
GAPDH	ATCCCATCACCATCTTCCAG	TGAGTCCTTCCACGATACCA
CCL2	AAGATCTCAGTGCAGAGGCTCG	CACAGATCTCCTTGGCCACAA
CD163	TTTGTCAACTTGAGTCCCTTCAC	TCCCGCTACACTTGTTTTCAC
CD206	GGGTTGCTATCACTCTCTATGC	TTTCTTGTCTGTTGCCGTAGTT
IL6	CCTTCGGTCCAGTTGCTTCT	CCAGTGCCTCTTTGCTGCTTTC

Evaluation of CCL2 by enzyme-linked immunosorbent assay (ELISA)

Approximately 5×10^5 cells were plated into 6-well plates. After the specified treatments according to the manufacturer's suggestions, the culture medium was harvested simultaneously. Detection of secreted human CCL2 was performed using h.MCP-1 ELISA kit (BOSTER, Wuhan, China, Lot: EK0441) according to the manufacturer's instructions.

Statistical analysis

All statistical analyses and graphical representations were performed in the R programming language (× 64, version 3.5.1), IBM SPSS Statistics 22 and GraphPad Prism 7 unless otherwise specified.

Results

HOXC6 was overexpressed in MSI-H CRC and led to poor prognosis

We previously revealed that HOXC6 was upregulated in RCC compared to LCC and normal colon tissues [7]. Then, we further explored the expression pattern of HOXC6 in MSI-H and MSS samples. Results showed that HOXC6 had the highest expression level in RCC MSI-H than in RCC MSS and LCC samples, suggesting that a close association of HOXC6 and MSI-H ($P < 0.001$, Fig. 1A).

Next, we assessed the prognostic value of HOXC6 based on TCGA and GSE39582 samples and found that high expression of HOXC6 was significantly associated with poor clinical outcome in MSI-H CRC (log rank $P = 0.02$, Fig. 1B).

HOXC6 recruited M2 macrophage infiltration via upregulating cytokine CCL2

To explore whether HOXC6 plays a role in the interaction between tumor cells and tumor microenvironment in CRC, we investigated in detail the functional phenotype under HOXC6 regulation. In this context, we compared the overall transcriptome variation between the HOXC6+ (mean RSEM: 133) and HOXC6- groups (mean RSEM: 12). There were 1,226 DEGs identified between the HOXC6 + and HOXC6- groups, most of which (1,001, 82%) were potentially upregulated by HOXC6 (Fig. 2A). For example, cytokines such as CCL2, CCL5, and IL6 had a much higher expression level in the HOXC6 + group (Fig. 2A). Furthermore, GO enrichment dissection revealed that these upregulated DEGs mainly participated in leukocyte migration ($P < 0.001$, FDR adjusted), extracellular matrix organization ($P < 0.001$), and leukocyte chemotaxis ($P < 0.001$, Fig. 2B). KEGG pathway enrichment also showed that cytokine – cytokine receptor interaction ($P < 0.001$), osteoclast differentiation ($P < 0.001$) and chemokine signaling pathway ($P < 0.001$, Fig. 2C) were the top enriched pathways, indicating that HOXC6 was positively linked to TME reshuffling. Thus, tumor purity was compared between the HOXC6 + and HOXC6- groups. Not surprisingly, tumor purity was significantly decreased in the HOXC6 + group ($P = 8.6E-5$, Wilcoxon test, Fig. 2D). To further determine the cell types accounting for the lower tumor purity in the HOXC6 + group, CIBERSORT was used to estimate the abundance of diverse cell types in CRC. We found that leukocytes were significantly increased in the HOXC6 + group ($P = 3.1E-5$, Wilcoxon test, Fig. 2D), and this difference was mainly due to M2 macrophage infiltration ($P = 0.02$, Wilcoxon test, Fig. 2D). Therefore, we speculated that M2 macrophages could be recruited into the tumor region by CCL2 under high levels of HOXC6.

To test this hypothesis, we experimentally investigated the relationship between HOXC6 and CCL2/M2 macrophage infiltration. First, we selected HCT116 cell line for HOXC6 overexpressed and knockdown cell line construction (Fig. S1A-C) because HCT116 belonging to one of the dMMR cell lines. At the mRNA level, CCL2 was elevated by 1.8-fold ($P < 0.05$, *t*-test) in the HCT116 HOXC6-OE group and decreased 41% ($P < 0.05$, *t*-test) in the HCT116 siHOXC6 group compared to the NC group (Fig. 3A). At the protein level, the CCL2 concentration in cell culture supernatants was elevated from 7.9 to 10.2 pg/ml ($P < 0.01$, *t*-test) by overexpressing HOXC6 in HCT116 cells (Fig. 3B). Furthermore, immunofluorescence was performed in 53 stage II RCC samples collected from the ZUCI cohort to evaluate M2 macrophage infiltration by the CD206-positive area (Fig. 3C). Through combined evaluation of HOXC6 and CD206, we confirmed a significantly positive correlation between M2 macrophage infiltration and HOXC6 expression ($P = 0.0002$, $r = 0.48$, Fig. 3D). In conclusion, these results revealed that upregulation of HOXC6 could recruit more macrophages by upregulating CCL2.

Overexpression of HOXC6 was associated with IL6/JAK pathway and EMT

Next, we explored the detailed molecular mechanism in the crosstalk between HOXC6 overexpressed tumors and M2 macrophages. GSEA was performed to identify prominent signatures associated with high HOXC6 expression. Interestingly, IL6/JAK/STAT3 signaling (NES = 1.78, $P = 0.014$, Fig. 4A) and EMT (NES = 1.71, $P = 0.038$, Fig. 4B) were characteristic of HOXC6 overexpression. Considering that HOXC6 was related to M2 macrophage infiltration by CCL2 and that cancer cell EMT could be induced by IL6

secreted from TAMs [14], we hypothesized that M2 macrophages induce EMT in tumor cells by regulating the IL6/HOXC6 axis.

M2 macrophages induced EMT of cancer cells by secreting IL6 and regulating the IL6/HOXC6 axis

To test our hypothesis, coculture assay was performed to examine the crosstalk between HCT116 cells and M2 macrophages. M2 macrophages were sequentially induced by PMA, IL4 and IL13 from progenitor THP-1 cells *in vitro* (Fig. 4C). CD163 and CD206, two M2 macrophage surface markers, were significantly upregulated in the induced M2 macrophages compared to THP-1cells (Fig. 4D). Then, the optimal coculture time for M2 macrophages/IL6 and tumor cells was determined to be 72 h/48 h according to the expression levels of HOXC6 (Fig. 4E and F). After 72 h coculture, the expression of IL6 in M2 macrophages was upregulated three-fold compared to that in M2 macrophages alone ($P < 0.01$, *t*-test, Fig. 4G). Furthermore, both the mRNA and protein levels of IL6 in M2 macrophages were significantly downregulated when coculture with ltv-shHOXC6 cells and upregulated by HOXC6-OE cells compared to shCtrl cells in the HCT116 cell background (Fig. 4H and I).

Next, the influence of M2 macrophages on tumor cells was also investigated. EMT of HCT116 cells was induced by downregulating ZO-1 and E-cadherin and upregulating snail, when coculturing with M2 macrophages, which was similar to coculture with human recombinant IL6 (Fig. 5A). In addition, HOXC6 could be upregulated when coculturing with M2 macrophages or IL6 only (Fig. 5A). When IL6 was knocked down in M2 macrophages, EMT was reversed and HOXC6 was downregulated as well (Fig. 5A). In addition, in spite of coculturing with M2 macrophages, MET was accomplished by knockdown of HOXC6 in HCT116 cells (Fig. 5B), indicating that HOXC6 played a critical role in metastasis. To test our hypothesis, we performed Transwell assay to evaluate whether HOXC6 could enhance the migration ability of tumor cells by inducing EMT. The results showed that the migration ability was greatly enhanced under high expression of HOXC6 (Fig. 5C and D), however, the proliferation ability of tumor cells remained unchanged (Fig. S2A and B). In summary, increased secretion of IL6 from M2 macrophages is the results of high HOXC6 expression in tumor cells and in turn M2 macrophages could induce EMT of tumor cells through the IL6/HOXC6 axis.

Blocking of IL6/HOXC6 axis is a promising strategy for MSI-H CRC treatment

In view of TAMs induce EMT via the IL6/HOXC6 axis, we next assessed whether blockade of HOXC6-oriented signaling pathway would be a feasible therapeutic regimen for CRC treatment. Given HOXC6 is not an approved druggable target so far, we explored whether inhibiting the IL6/JAK pathway was a potential alternative therapeutic schedule for HOXC6-overexpressed MSI-H CRC. Interestingly, ruxolitinib, a selective JAK1/2 inhibitor, inhibited tumor cell EMT by upregulating E-cadherin and downregulating snail and HOXC6 in a dose-dependent manner (Fig. 6A). Moreover, HOXC6 was downregulated by ruxolitinib despite the presence of IL6 (Fig. 6B). Furthermore, IL6 could not upregulate HOXC6 and snail nor downregulate E-cadherin when ruxolitinib existence. These results indicated that HOXC6 could be indirectly druggable by ruxolitinib.

Discussion

In this study, HOXC6 was confirmed to be overexpressed in MSI-H CRC and associated with poor prognosis, which is in line with previous studies in other cancer types [15–17]. As a heterogeneous ecosystem, tumors are composed of various components, such as diverse stromal cells and lymphocytes [18]. Deconvolution of 22 lymphocytes in tumor tissue using CIBERSORT revealed a significant enrichment of M2 macrophages in HOXC6 high-expression groups in CRC. TAMs are the main component of infiltrated immune cells in TME [19] and have been shown to play an important role in tumorigenesis [20], angiogenesis [21, 22], metastasis [23, 24], and chemoresistance [25–30]. Here, we first reported the reciprocal interaction of HOXC6 between CRC and TAMs. We found that cytokine CCL2, a known strong monocyte-attracting cytokine that recruits macrophages to the tumor region, could be upregulated by HOXC6. Furthermore, IL6 was upregulated in macrophages by coculture with HOXC6-OE CRC cells and *vice versa*. IL6 secreted by macrophages was associated with EMT of tumor cells, which was consistent with a previous study [14]. Additionally, IL6 secreted by TAM has various effect on tumor cells, such as promotes expansion of human hepatocellular carcinoma stem cells [31] and cancer immune evasion [32]. In summary, we first found that high expression of HOXC6 could attract more macrophages into the tumor area by promoting CCL2 secretion, which in turn resulted in upregulation of HOXC6 in tumor cells via IL6 secreted from macrophages (Fig. 6C).

With regard to the downstream regulatory cascade of HOXC6 participating in CRC progression, we found high expression of HOXC6 was significantly associated with IL6/JAK/STAT3 pathway and subsequent EMT of CRC cells, and targeting JAK not only inhibited EMT but also downregulated HOXC6, which indicated that the potential IL6/JAK/HOXC6 axis present in CRC. In view of there is no HOXC6-derived drug currently, targeting IL6/IL6R or JAK is a feasible strategy to block the positive crosstalk for HOXC6 overexpressed or high TAM infiltrated CRC patients, such as sarilumab (IL6R inhibitor) approved by the FDA for castleman syndrome treatment [33] and ruxolitinib (JAK1/2 inhibitor) approved by the FDA for myelofibrosis in 2011 [34].

Conclusion

In conclusion, the most important finding in this study is high expression of HOXC6 attracts more M2 macrophage infiltration via upregulating CCL2 and M2 macrophages induced EMT of cancer cells by regulating IL6/HOXC6 axis. In addition, block IL6/JAK pathway accompanied by downregulating HOXC6 and inhibiting EMT, which provided an alternative therapy strategy for indirectly targeting HOXC6. Consequently, HOXC6 could serve as a biomarker for CRC metastatic potential predicting and a drug target but warrant further investigation.

Abbreviations

cell counting Kit-8 (CCK8)

colorectal cancer (CRC)

differentially expressed genes (DEGs)

epithelial-mesenchymal transition (EMT)

false discovery rate (FDR)

Gene Expression Omnibus (GEO)

gene ontology (GO)

gene set enrichment analysis (GSEA)

kyoto encyclopedia of genes and genomes (KEGG)

left-sided colon cancer (LCC)

microsatellite instability-high (MSI-H)

microsatellite stable (MSS)

right-sided colon cancer (RCC)

The Cancer Genome Atlas (TCGA)

tumor microenvironment (TME)

Zhejiang University Cancer Institute (ZUCI)

Declarations

Ethics approval and consent to participate

This study was approved by the Ethics Committee of the Second Affiliated Hospital, Zhejiang University School of Medicine.

Consent for publication

All authors read and are consent for the publication of this manuscript.

Availability of data and materials

The datasets used during the current study are available from the corresponding author on reasonable request.

Competing interests

The authors declare that they have no competing interests.

Funding

This work was supported by National Natural Science Foundation of China (grant number: 81802883) and Fundamental Research Funds for the Central Universities (grant number: 2018FZA7012) to WXH.

Authors' contributions

LNQ, WXH and SZ designed the study. WXH performed GO, KEGG, and GSEA analysis. LNQ and KLX performed western blots. LNQ performed qRT-PCR, CCK8, Transwell, and ELISA. BTZ, KLW and JNC performed mouse experiments. BTZ collected the human tissue samples. WXH performed the IHC and IF assays. JNC performed statistical analysis. LNQ, BTZ and WXH wrote the manuscript. All authors read and approved the final manuscript.

Acknowledgments

Not applicable.

References

1. *Siegel*, *R.L.*, *K.D. Miller*, and J. A., *Cancer statistics*, *2019*. *CA Cancer J Clin.*, *2019*. *69*(*1*): p. *7–34*.
2. *Dienstmann*, *R.*, et al., *Consensus molecular subtypes and the evolution of precision medicine in colorectal cancer*. *Nat Rev Cancer*, *2017*. *17*(*2*): p. *79–92*.
3. *Hansen*, *I.O.* and *P. Jess*, *Possible better long-term survival in left versus right-sided colon cancer - a systematic review*. *Dan Med J*, *2012*. *59*(*6*): p. *A4444*.
4. *Yang*, *S.Y.*, *M.S. Cho*, and *N.K. Kim*, *Difference between right-sided and left-sided colorectal cancers: from embryology to molecular subtype*. *Expert Rev Anticancer Ther*, *2018*. *18*(*4*): p. *351–358*.
5. *Le*, *D.T.*, et al., *PD-1 Blockade in Tumors with Mismatch-Repair Deficiency*. *N Engl J Med*, *2015*. *372*(*26*): p. *2509-20*.
6. *Orecchioni*, *S.*, et al., *Vinorelbine, cyclophosphamide and 5-FU effects on the circulating and intratumoural landscape of immune cells improve anti-PD-L1 efficacy in preclinical models of breast cancer and lymphoma*. *Br J Cancer*, *2018*. *118*(*10*): p. *1329–1336*.
7. *Hu*, *W.*, et al., *Multi-omics Approach Reveals Distinct Differences in Left- and Right-Sided Colon Cancer*. *Mol Cancer Res*, *2018*. *16*(*3*): p. *476–485*.
8. *Hu*, *W.*, et al., *Subtyping of microsatellite instability-high colorectal cancer*. *Cell Commun Signal*, *2019*. *17*(*1*): p. *79*.
9. *Yu*, *G.*, et al., *clusterProfiler: an R package for comparing biological themes among gene clusters*. *Omics*, *2012*. *16*(*5*): p. *284-7*.
10. *Subramanian*, *A.*, et al., *Gene set enrichment analysis: a knowledge-based approach for interpreting genome-wide expression profiles*. *Proc Natl Acad Sci U S A*, *2005*. *102*(*43*): p. *15545-50*.

11. *Mootha, V.K.*, et al., *PGC-1alpha-responsive genes involved in oxidative phosphorylation are coordinately downregulated in human diabetes*. *Nat Genet*, *2003*. *34*(*3*): p. *267 – 73*.
12. *Newman, A.M.*, et al., *Robust enumeration of cell subsets from tissue expression profiles*. *Nat Methods*, *2015*. *12*(*5*): p. *453-7*.
13. *Aran, D., M. Sirota*, and *A.J. Butte, Systematic pan-cancer analysis of tumour purity*. *Nat Commun*, *2015*. *6*: p. *8971*.
14. *Wei, C.*, et al., *Crosstalk between cancer cells and tumor associated macrophages is required for mesenchymal circulating tumor cell-mediated colorectal cancer metastasis*. *Mol Cancer*, *2019*. *18*(*1*): p. *64*.
15. *Zhang, F.*, et al., *HOXC6 gene silencing inhibits epithelial-mesenchymal transition and cell viability through the TGF-beta/smad signaling pathway in cervical carcinoma cells*. *Cancer Cell Int*, *2018*. *18*: p. *204*.
16. *Chen, S.W.*, et al., *HOXC6 promotes gastric cancer cell invasion by upregulating the expression of MMP9*. *Mol Med Rep*, *2016*. *14*(*4*): p. *3261-8*.
17. *Hamid, A.R.*, et al., *The role of HOXC6 in prostate cancer development*. *Prostate*, *2015*. *75*(*16*): p. *1868-76*.
18. *Van den Eynde, M.*, et al., *The Link between the Multiverse of Immune Microenvironments in Metastases and the Survival of Colorectal Cancer Patients*. *Cancer Cell*, *2018*. *34*(*6*): p. *1012–1026.e3*.
19. *Morrison, C., Immuno-oncologists eye up macrophage targets*. *Nat Rev Drug Discov*, *2016*. *15*(*6*): p. *373-4*.
20. *Schwitalla, S.*, et al., *Intestinal tumorigenesis initiated by dedifferentiation and acquisition of stem-cell-like properties*. *Cell*, *2013*. *152*(*1–2*): p. *25–38*.
21. *Murdoch, C.*, et al., *The role of myeloid cells in the promotion of tumour angiogenesis*. *Nat Rev Cancer*, *2008*. *8*(*8*): p. *618 – 31*.
22. *Valkovic, T.*, et al., *Correlation between vascular endothelial growth factor, angiogenesis, and tumor-associated macrophages in invasive ductal breast carcinoma*. *Virchows Arch*, *2002*. *440*(*6*): p. *583-8*.
23. *Pollard, J.W., Tumour-educated macrophages promote tumour progression and metastasis*. *Nat Rev Cancer*, *2004*. *4*(*1*): p. *71 – 8*.
24. *Fan, Q.M.*, et al., *Tumor-associated macrophages promote cancer stem cell-like properties via transforming growth factor-beta1-induced epithelial-mesenchymal transition in hepatocellular carcinoma*. *Cancer Lett*, *2014*. *352*(*2*): p. *160-8*.
25. *Yang, J.*, et al., *Tumor-associated macrophages regulate murine breast cancer stem cells through a novel paracrine EGFR/Stat3/Sox-2 signaling pathway*. *Stem Cells*, *2013*. *31*(*2*): p. *248 – 58*.
26. *Dijkgraaf, E.M.*, et al., *Chemotherapy alters monocyte differentiation to favor generation of cancer-supporting M2 macrophages in the tumor microenvironment*. *Cancer Res*, *2013*. *73*(*8*): p. *2480-92*.

27. *Mantovani, A.* and *P. Allavena, The interaction of anticancer therapies with tumor-associated macrophages. J Exp Med, 2015. 212(4)*: p. *435 – 45.*
28. *Shojaei, F.*, et al., *Tumor refractoriness to anti-VEGF treatment is mediated by CD11b + Gr1 + myeloid cells. Nat Biotechnol, 2007. 25(8)*: p. *911 – 20.*
29. *Shree, T.*, et al., *Macrophages and cathepsin proteases blunt chemotherapeutic response in breast cancer. Genes Dev, 2011. 25(23)*: p. *2465-79.*
30. *Paulus, P.*, et al., *Colony-stimulating factor-1 antibody reverses chemoresistance in human MCF-7 breast cancer xenografts. Cancer Res, 2006. 66(8)*: p. *4349-56.*
31. *Wan, S.*, et al., *Tumor-associated macrophages produce interleukin 6 and signal via STAT3 to promote expansion of human hepatocellular carcinoma stem cells. Gastroenterology, 2014. 147(6)*: p. *1393 – 404.*
32. *Chan, L.C.*, et al., *IL-6/JAK1 pathway drives PD-L1 Y112 phosphorylation to promote cancer immune evasion. J Clin Invest, 2019. 129(8)*: p. *3324–3338.*
33. *Ascierto, P.A.*, et al., *Insights from immuno-oncology: the Society for Immunotherapy of Cancer Statement on access to IL-6-targeting therapies for COVID-19. Journal for ImmunoTherapy of Cancer, 2020. 8(1)*: p. *e000878.*
34. *FDA*, https://www.accessdata.fda.gov/drugsatfda_docs/label/2011/202192lbl.pdf. *2011.*

Figures

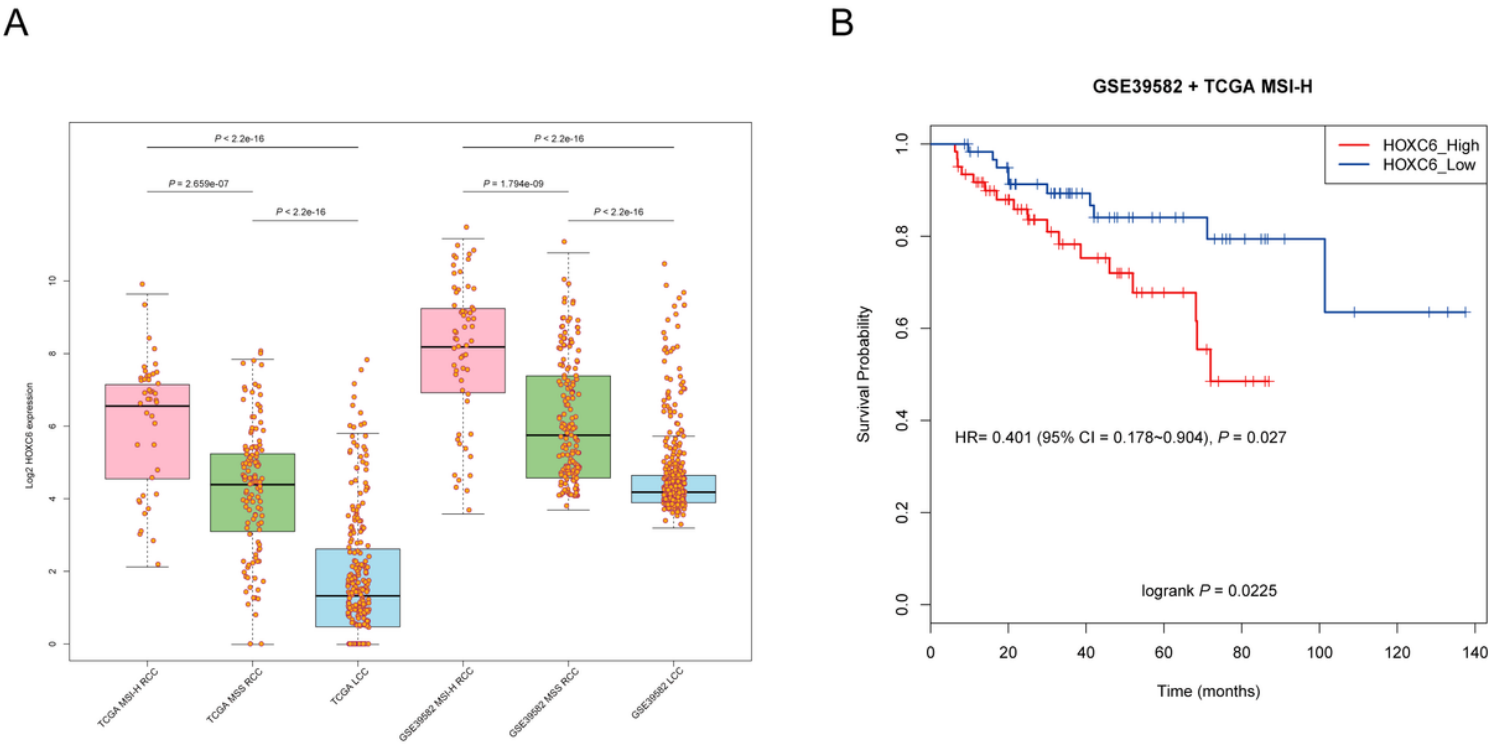

Figure 1

Expression of HOXC6 and prognostic value in CRC. A. HOXC6 was overexpressed in MSI-H RCC compared to MSS RCC and LCC in both TCGA and GSE39582 datasets. B. KM plot showed that the HOXC6 high-expression group had a poor prognosis compared to the low-expression group in MSI-H CRC.

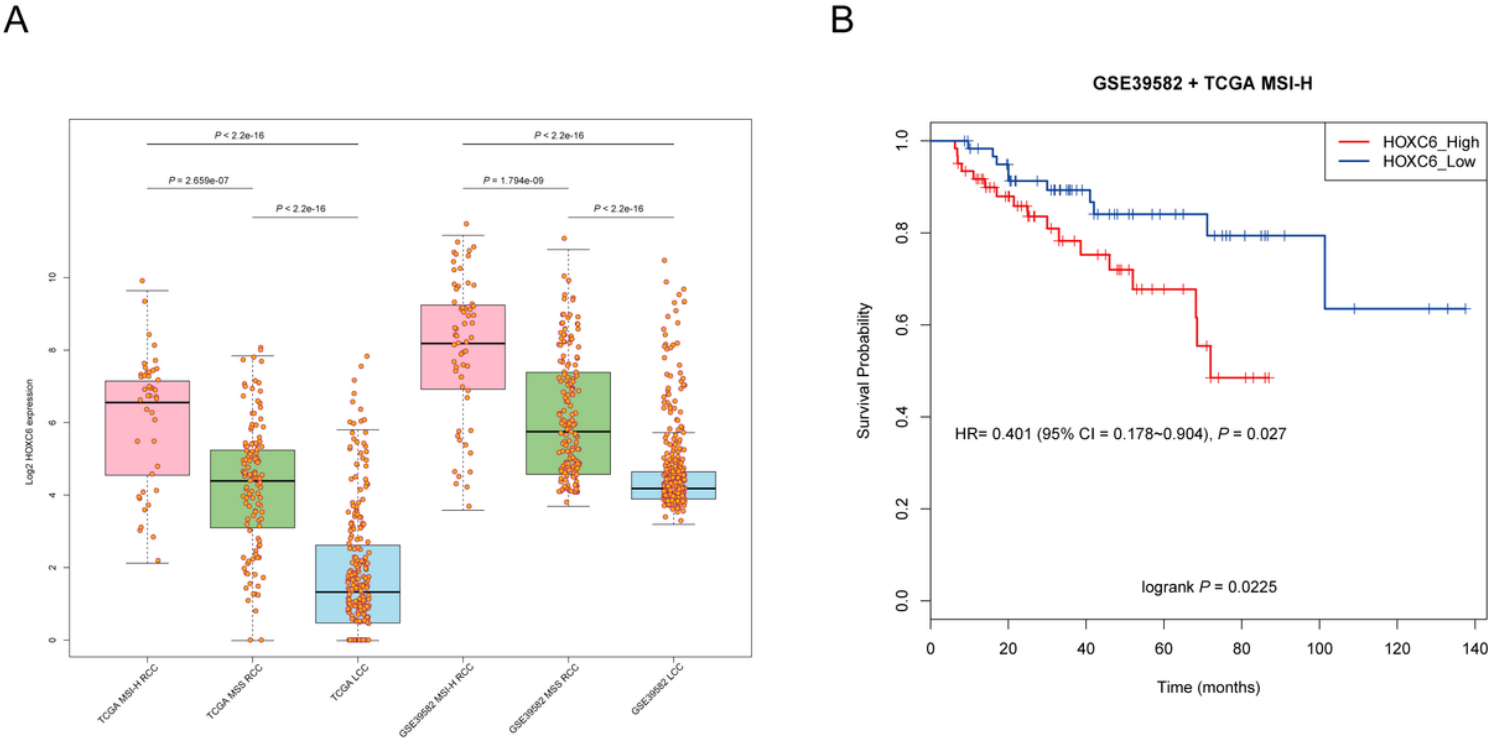

Figure 1

Expression of HOXC6 and prognostic value in CRC. A. HOXC6 was overexpressed in MSI-H RCC compared to MSS RCC and LCC in both TCGA and GSE39582 datasets. B. KM plot showed that the HOXC6 high-expression group had a poor prognosis compared to the low-expression group in MSI-H CRC.

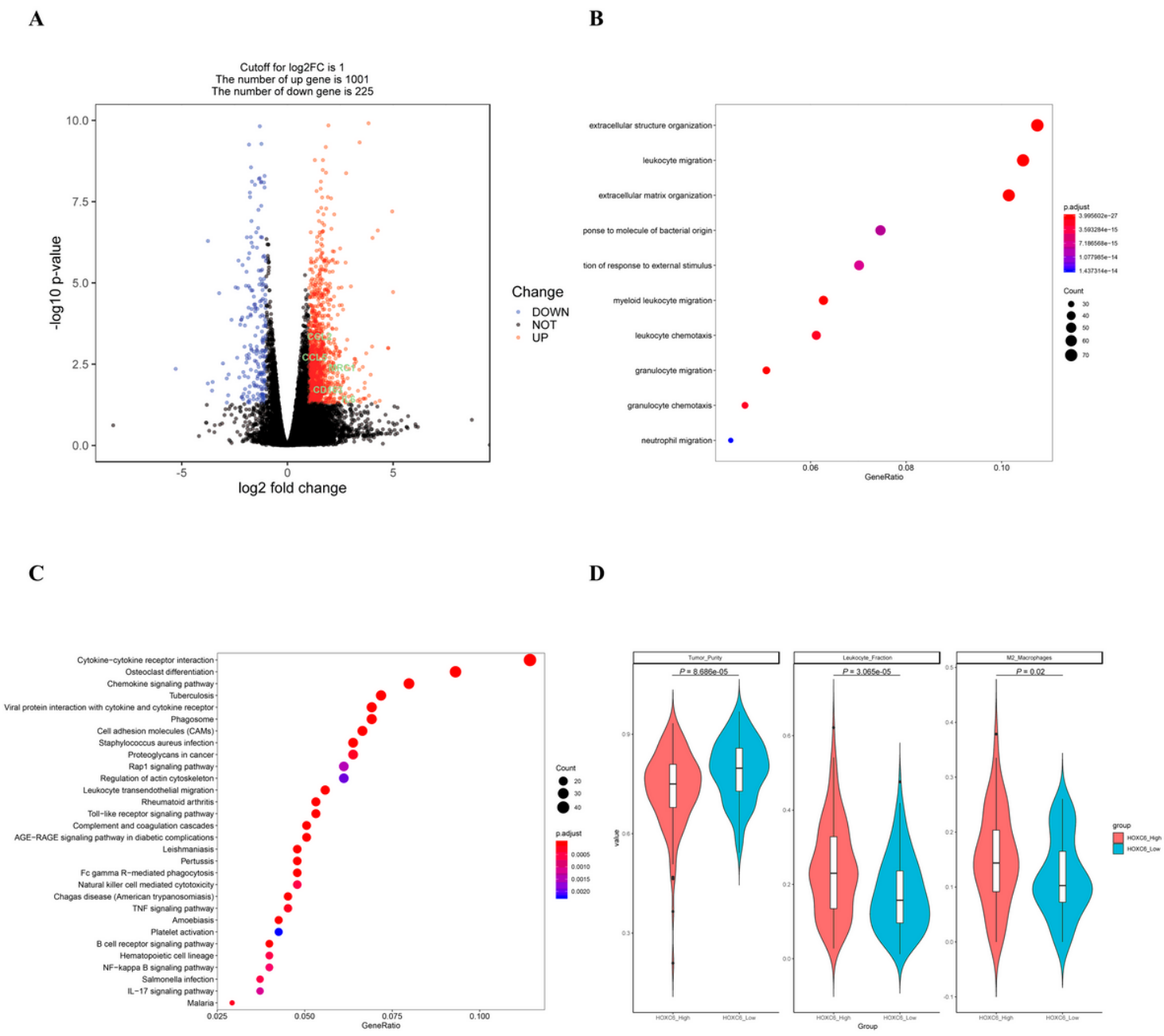

Figure 2

HOXC6 was correlated with elevated cytokine interaction and TME reshuffling. A. Volcano plot of DEGs identified between the HOXC6 low- and high-expression groups using TCGA samples. B. GO enrichment of DEGs in the HOXC6 high-expression group using TCGA samples. C. KEGG pathway enrichment of DEGs in the HOXC6 high-expression group using TCGA samples. D. Tumor purity, leukocyte fraction, and M2 macrophage infiltration were compared between HOXC6 high- and low-expression groups.

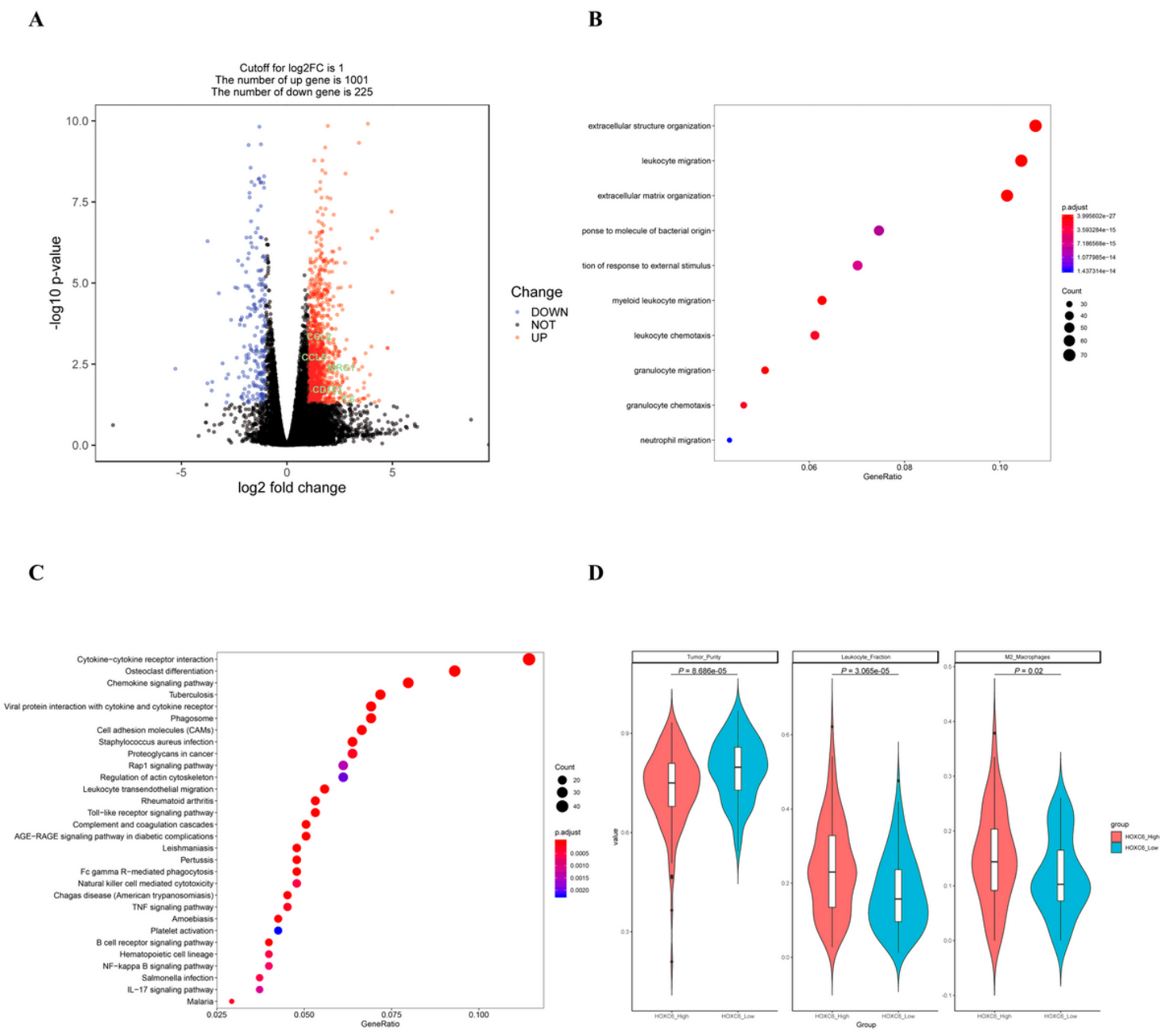

Figure 2

HOXC6 was correlated with elevated cytokine interaction and TME reshuffling. A. Volcano plot of DEGs identified between the HOXC6 low- and high-expression groups using TCGA samples. B. GO enrichment of DEGs in the HOXC6 high-expression group using TCGA samples. C. KEGG pathway enrichment of DEGs in the HOXC6 high-expression group using TCGA samples. D. Tumor purity, leukocyte fraction, and M2 macrophage infiltration were compared between HOXC6 high- and low-expression groups.

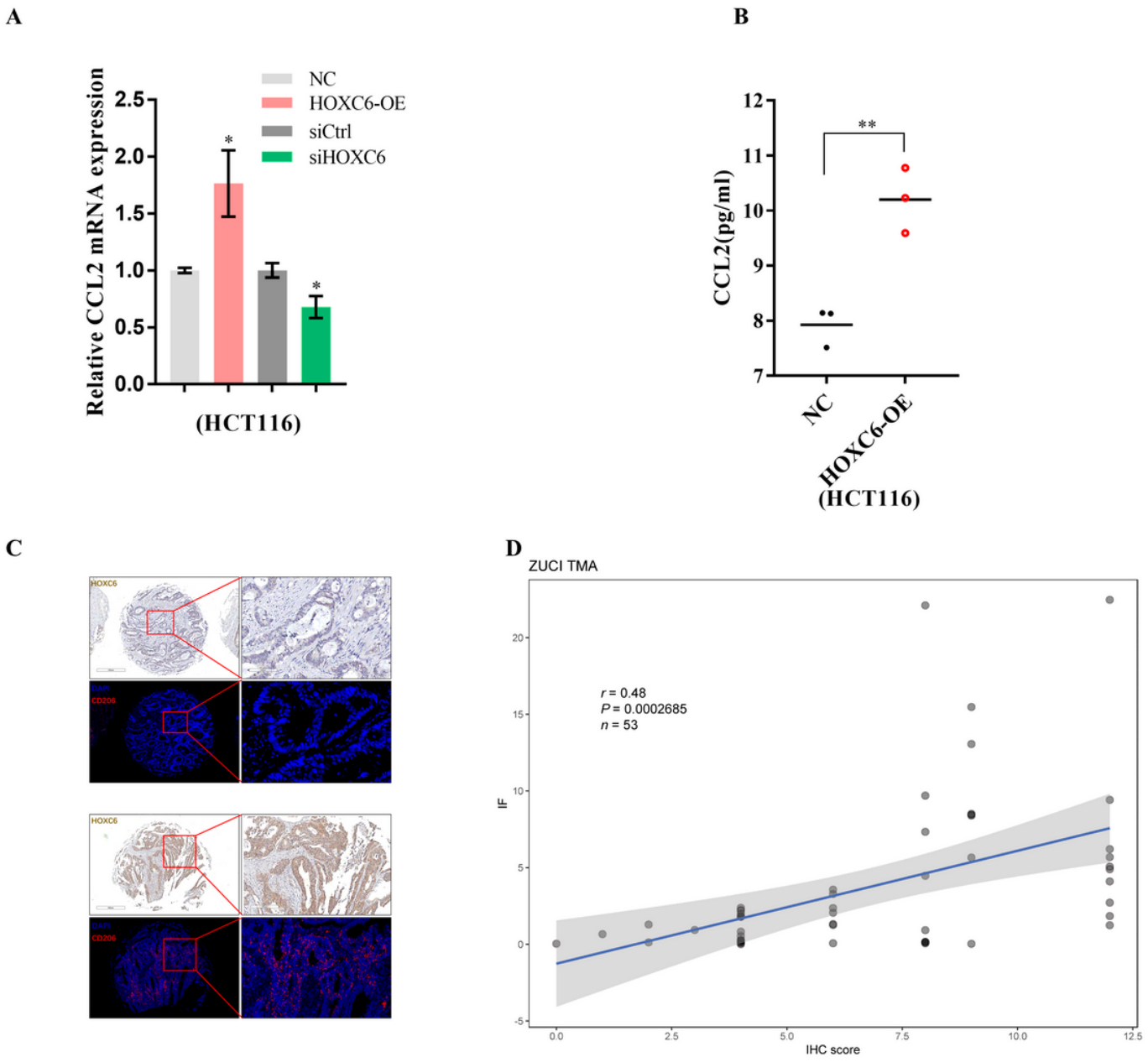

Figure 3

HOXC6 was correlated with elevated CCL2 and increased M2 macrophage infiltration. A. Relative mRNA expression of CCL2 in the HOXC6-OE and siHOXC6 group compared to NC group in HCT116 cells. B. ELISA detection of CCL2 concentrations in HOXC6-OE group compared to NC group using HCT116 cell supernatants. C. Representative images of HOXC6 low-expression/M2 macrophage low-infiltration samples and HOXC6 high-expression/M2 macrophage high-infiltration samples. D. Correlation between HOXC6 expression and M2 macrophage infiltration in 53 stage II RCC samples from the ZUCI cohort. *: P < 0.05; **: P < 0.01; ***: P < 0.001.

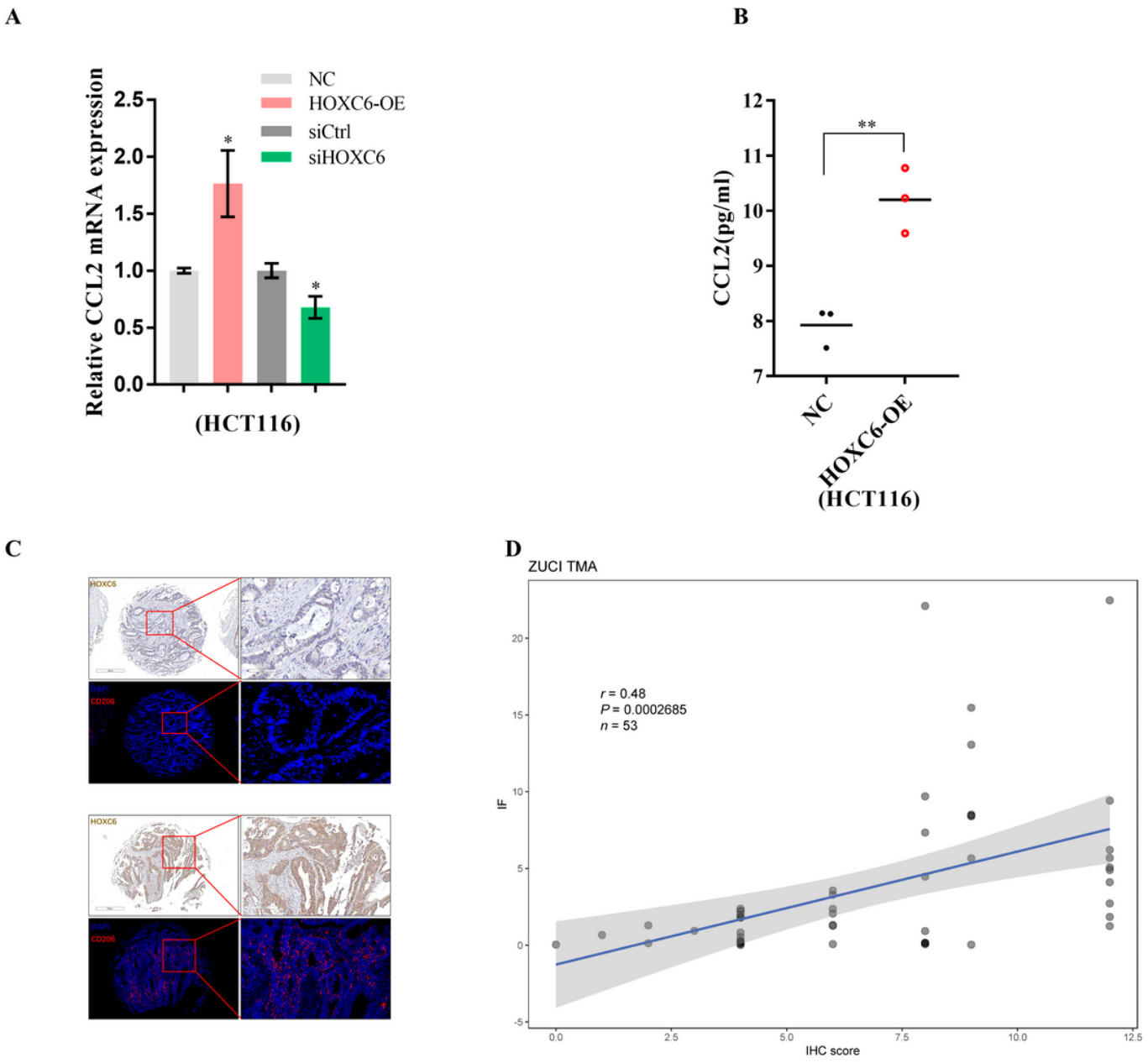

Figure 3

HOXC6 was correlated with elevated CCL2 and increased M2 macrophage infiltration. A. Relative mRNA expression of CCL2 in the HOXC6-OE and siHOXC6 group compared to NC group in HCT116 cells. B. ELISA detection of CCL2 concentrations in HOXC6-OE group compared to NC group using HCT116 cell supernatants. C. Representative images of HOXC6 low-expression/M2 macrophage low-infiltration samples and HOXC6 high-expression/M2 macrophage high-infiltration samples. D. Correlation between HOXC6 expression and M2 macrophage infiltration in 53 stage II RCC samples from the ZUCI cohort. *: P < 0.05; **: P < 0.01; ***: P < 0.001.

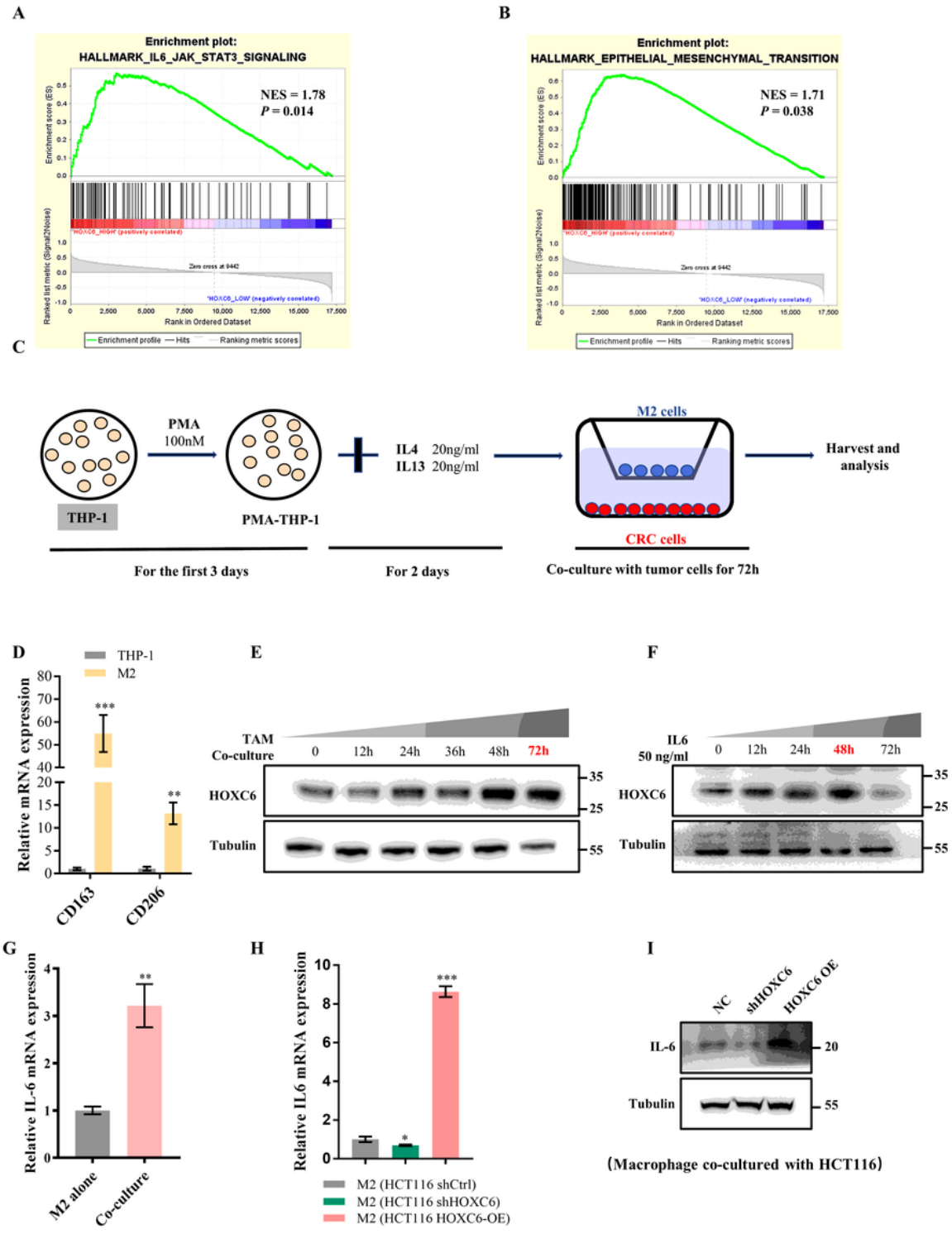

Figure 4

M2 macrophage induced from THP-1 cells in vitro and coculturing of M2 macrophages and HCT116 cells. A and B. GSEA showed that the IL6/JAK/STAT3 pathway and EMT process were significantly enriched in the HOXC6-overexpressing group. C. Flow chart of M2 macrophages induced from THP-1 cells and schematic diagram for coculturing of M2 macrophages and tumor cells. D. Relative mRNA expression of CD163 and CD206 in induced M2 macrophages and THP-1 cells. E. Protein expression of

HOXC6 in HCT116 cells cocultured with M2 macrophages over a time period from 0 to 72h. F. Protein expression of HOXC6 in HCT116 cells cocultured with 50ng/ml IL6 over a time period from 0 to 72h. G. Relative mRNA expression of IL6 in M2 macrophages with and without coculture with HCT116 cells. H. Relative mRNA expression of IL6 in M2 macrophages cocultured with shCtrl, shHOXC6, or HOXC6-OE HCT116 cells. I. Protein expression of IL6 in M2 macrophages cocultured with shCtrl, shHOXC6, and HOXC6-OE cells.

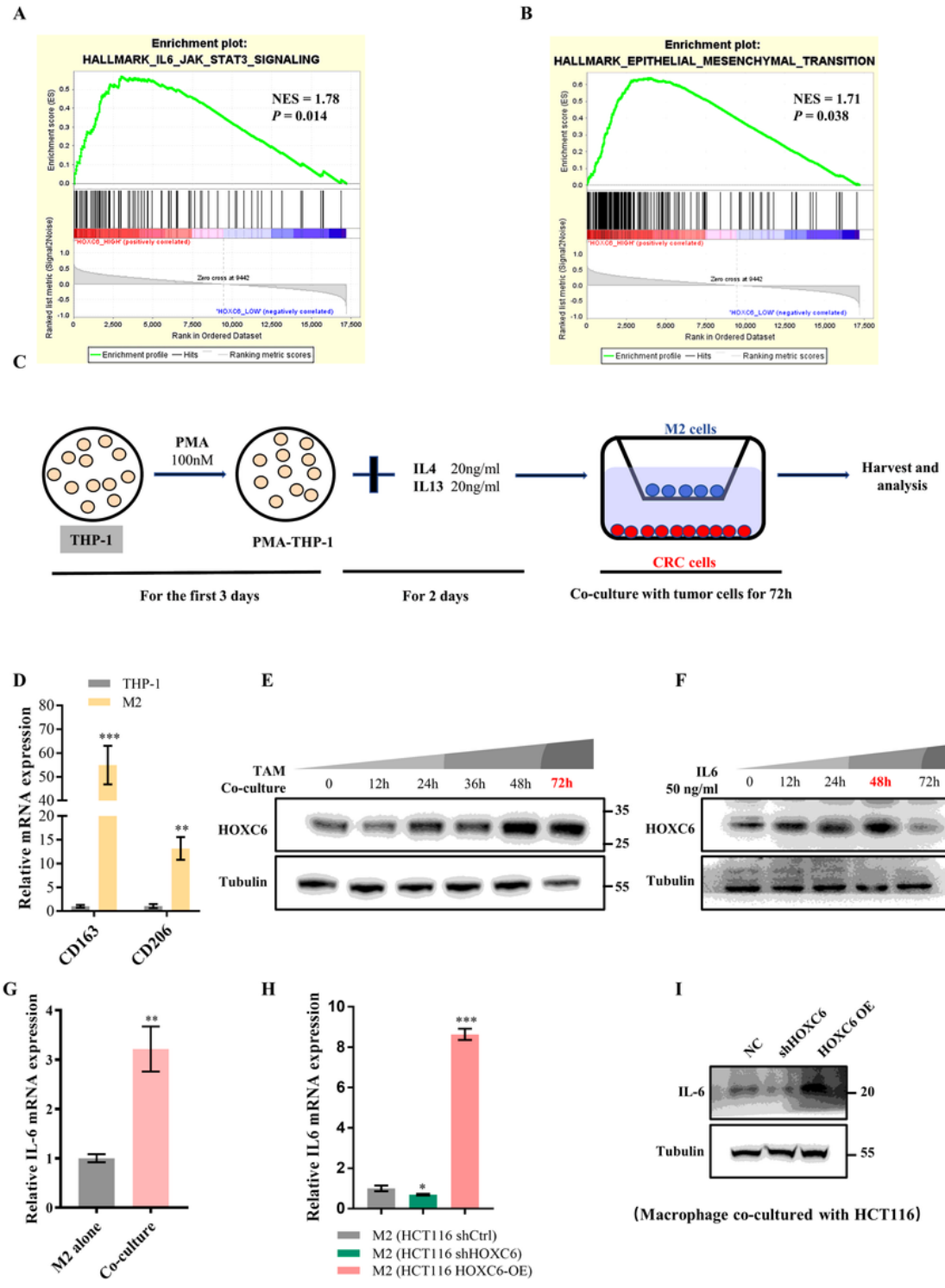

Figure 4

M2 macrophage induced from THP-1 cells in vitro and coculturing of M2 macrophages and HCT116 cells. A and B. GSEA showed that the IL6/JAK/STAT3 pathway and EMT process were significantly enriched in the HOXC6-overexpressing group. C. Flow chart of M2 macrophages induced from THP-1 cells and schematic diagram for coculturing of M2 macrophages and tumor cells. D. Relative mRNA expression of CD163 and CD206 in induced M2 macrophages and THP-1 cells. E. Protein expression of HOXC6 in HCT116 cells cocultured with M2 macrophages over a time period from 0 to 72h. F. Protein expression of HOXC6 in HCT116 cells cocultured with 50ng/ml IL6 over a time period from 0 to 72h. G. Relative mRNA expression of IL6 in M2 macrophages with and without coculture with HCT116 cells. H. Relative mRNA expression of IL6 in M2 macrophages cocultured with shCtrl, shHOXC6, or HOXC6-OE HCT116 cells. I. Protein expression of IL6 in M2 macrophages cocultured with shCtrl, shHOXC6, and HOXC6-OE cells.

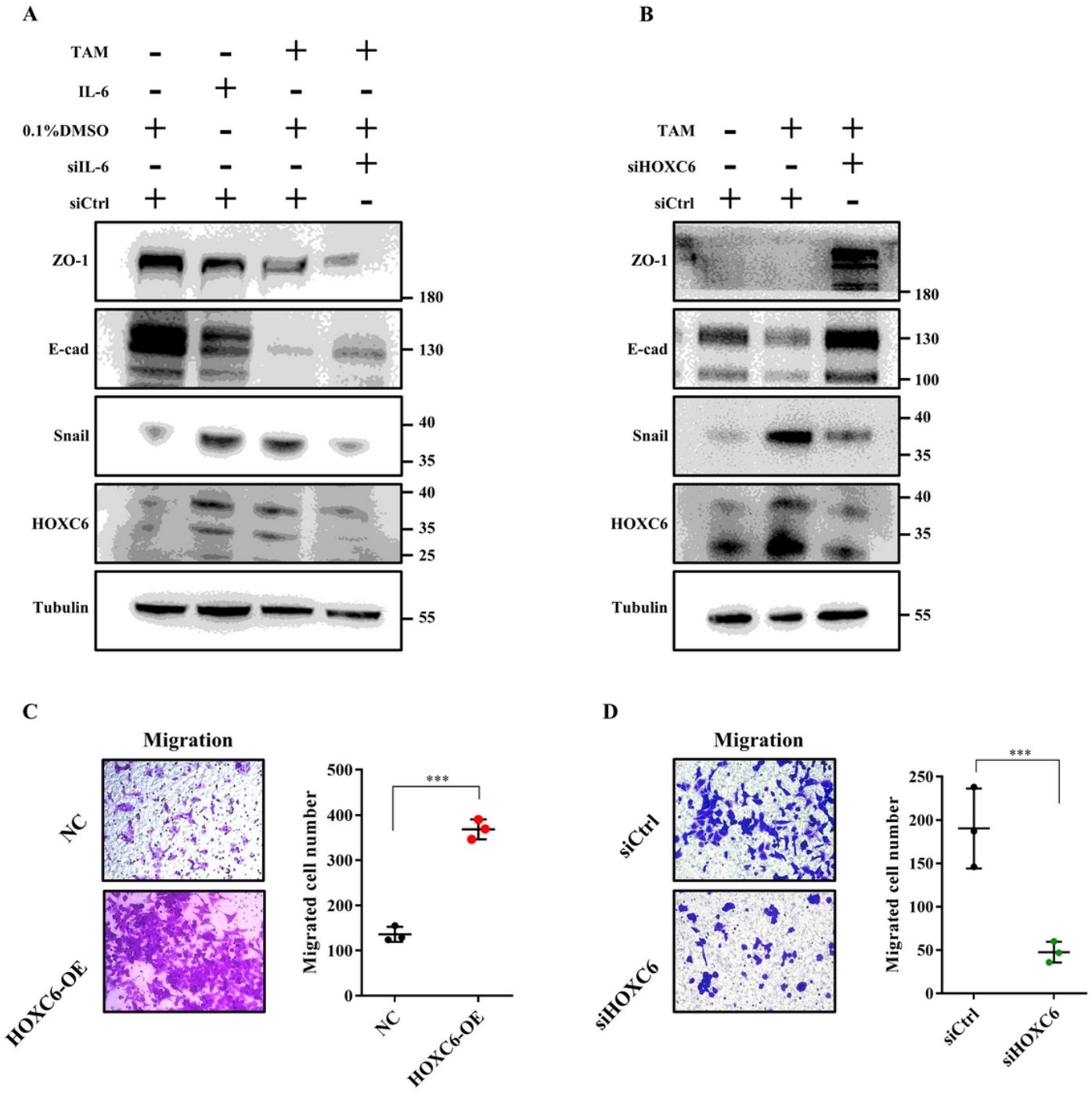

Figure 5

M2 macrophages induced EMT of cancer cells by secreting IL6 and regulating the IL6/HOXC6 axis. A. Protein expression of ZO-1, E-cadherin, snail, and HOXC6 in four different treated HCT116 groups. B. Protein expression of ZO-1, E-cadherin, Snail, and HOXC6 in three different treated HCT116 groups. C. Transwell experiments without matrigel in NC and HOXC6-OE HCT116 groups. D. Transwell experiments without matrigel in siCtrl and siHOXC6 HCT116 groups. ***: $P < 0.001$; n.s.: no significance.

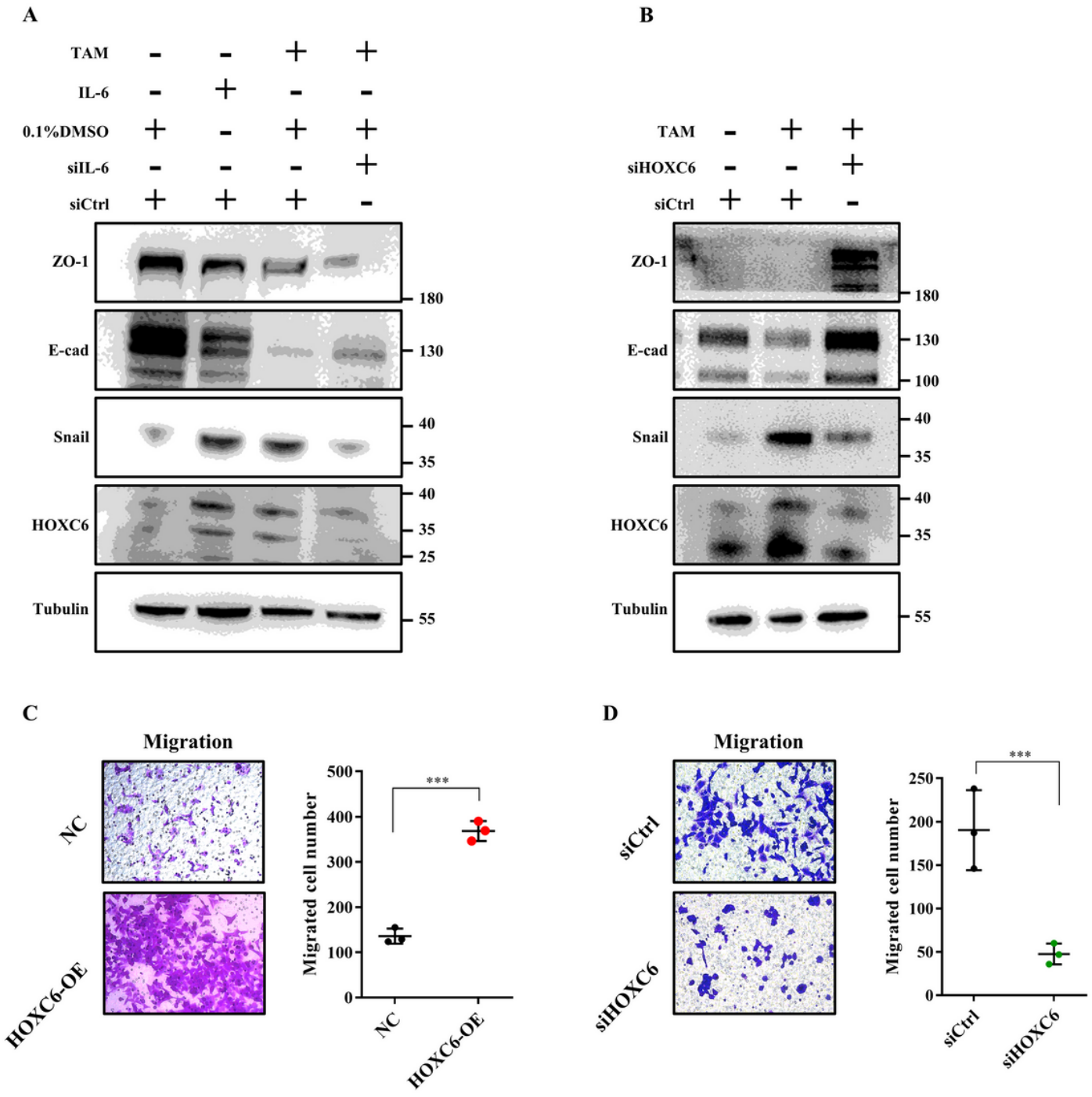

Figure 5

M2 macrophages induced EMT of cancer cells by secreting IL6 and regulating the IL6/HOXC6 axis. A. Protein expression of ZO-1, E-cadherin, snail, and HOXC6 in four different treated HCT116 groups. B. Protein expression of ZO-1, E-cadherin, Snail, and HOXC6 in three different treated HCT116 groups. C. Transwell experiments without matrigel in NC and HOXC6-OE HCT116 groups. D. Transwell experiments without matrigel in siCtrl and siHOXC6 HCT116 groups. ***: $P < 0.001$; n.s.: no significance.

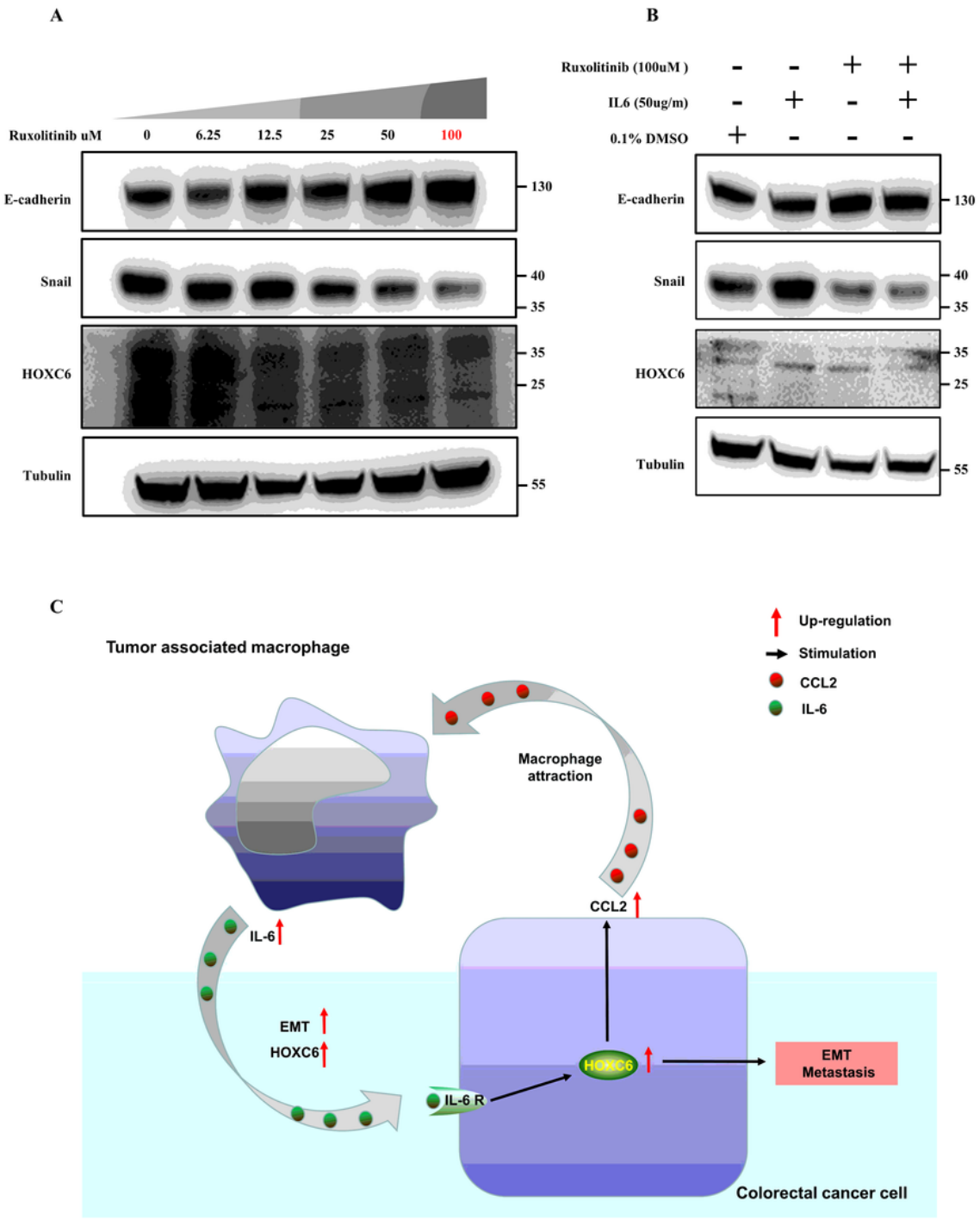

Figure 6

Inhibition of IL6/JAK pathway by ruxolitinib downregulates HOXC6 and inhibits EMT. A. The expression of E-cadherin, snail and HOXC6 in HCT116 cells treated with increasing the concentration of ruxolitinib. B. The expression of E-cadherin, snail and HOXC6 in four different treatment groups of HCT116 cells. C. Schematic diagram of the interactions of HOXC6-OE tumor cells with TAMs in CRC.

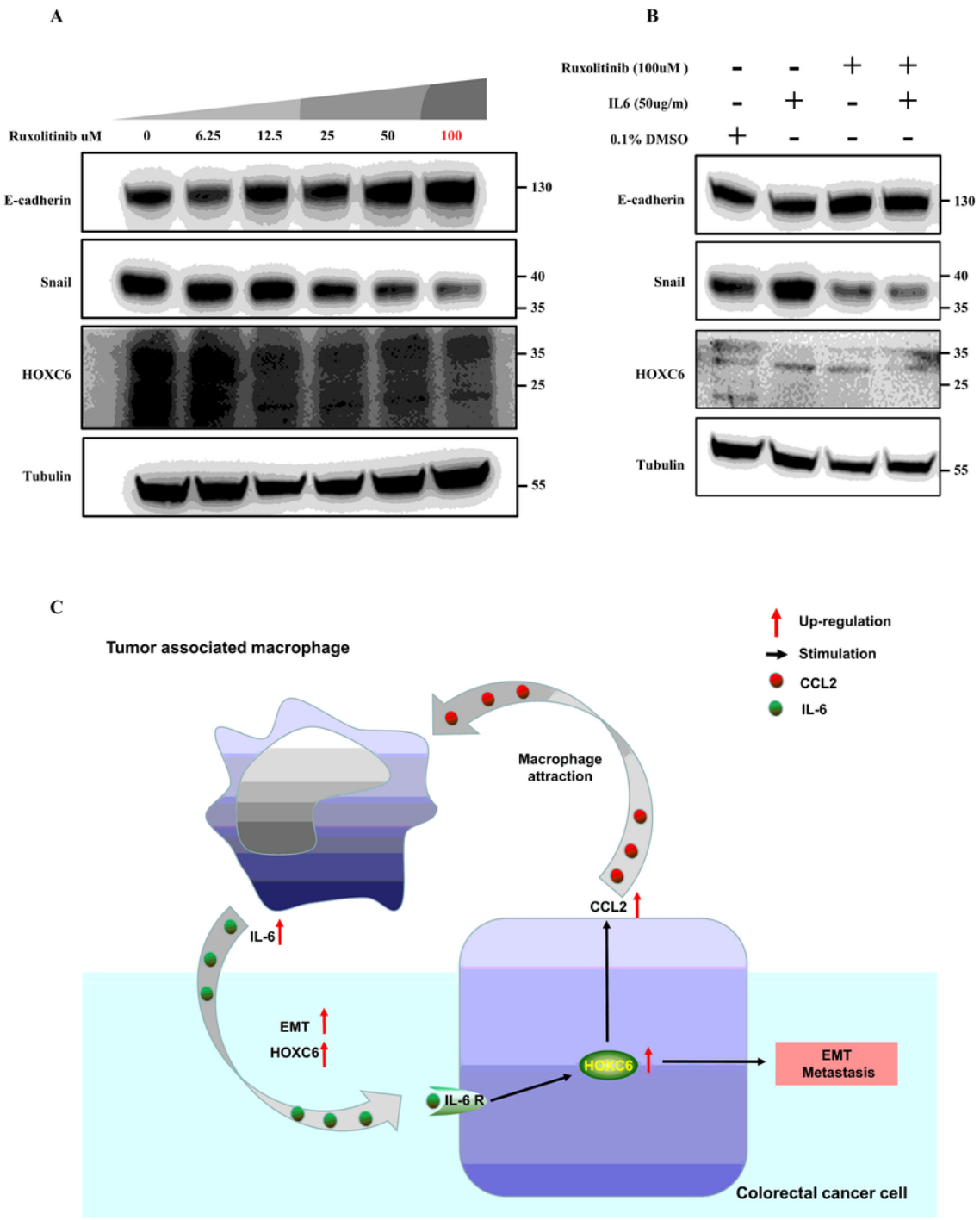

Figure 6

Inhibition of IL6/JAK pathway by ruxolitinib downregulates HOXC6 and inhibits EMT. A. The expression of E-cadherin, snail and HOXC6 in HCT116 cells treated with increasing the concentration of ruxolitinib. B. The expression of E-cadherin, snail and HOXC6 in four different treatment groups of HCT116 cells. C. Schematic diagram of the interactions of HOXC6-OE tumor cells with TAMs in CRC.

Supplementary Files

This is a list of supplementary files associated with this preprint. Click to download.

- FigureS1.tif
- FigureS1.tif
- FigureS2.tif
- FigureS2.tif